

Rocking by rolling: super-fast near-collisional dynamics of perturbed vertical cylinders

Manoj Srinivasan*

*Theoretical and Applied Mechanics,
Cornell University, NY 14853*

*Current address: Mechanical and Aerospace Engineering,
Princeton University, NJ 08544*

(Dated: January 15, 2007)

A slightly tilted vertical cylinder on a table-top rights itself, coming to a halt after “rocking” for a while. These rocking motions may involve collisions of the cylinder’s circular bottom surface with the table-top. Here we study the more likely motions that almost but do not quite involve a face-down collision of the cylinder’s bottom with the table-top. For ideal cylinders that can roll without slip or slide without friction on their circular bottoms, the typical rocking motions do not involve collisions. Instead, they involve slow inverted pendulum-like motions interrupted by infinitely fast rolling or sliding motions during which the contact point with the table shifts by a finite angle in infinitesimal time. We derive simple asymptotic formulas for this “angle of turn” of the contact point for two simple cases: sliding without friction and rolling without slip. These formulas for the angle of turn depend only on the properties of the cylinder and the assumed friction law. These results explain why not-too-tall cylinders or disks never seem to rock symmetrically on diametrically opposite ends. Also, on the other hand, very tall cylinders that appear to rock back and forth on diametrically opposite points on the bottom rim are really (often) rolling and/or sliding very quickly on the rim by a little over 180 degrees.

PACS numbers: 45.20.dc,45.40.-f

I. INTRODUCTION

Consider a cylinder, a body of revolution, with a planar circular bottom, standing vertically on a horizontal tabletop so that the planar circular bottom of the cylinder is in contact with the table. Now tilt the cylinder by a small angle and gently let go, with exactly zero initial angular velocity. The cylinder will right itself, but in the process fall flat on its bottom. What happens next? Generally, the cylinder comes to a quick halt after a little bit of “rocking” on its circular bottom rim. During this rocking motion, too much energy is lost too quickly for anything interesting to be noticed by the naked eye.

To aid the eye, we perform a slightly different experiment (see video [9]), whose typical result is shown in Fig. 1. Instead of gently letting go of the slightly tilted cylinder, we flick the cylinder’s top forward with our fingers so as to provide a righting angular velocity – that is, an angular velocity exactly along the axis about which the cylinder is tilted, making sure that the angular velocity is not so high that the cylinder leaves the table as it pivots over. The cylinder, as before, first becomes (almost) vertical as it rotates like an inverted pendulum about the initial contact point A (assuming no slip), its bottom face apparently colliding with the table. After a brief interaction with the table, the cylinder falls over onto the other side, rotating like an inverted pendulum

in a vertical plane about a new contact point B. When this experiment is performed with a cylinder that is not too tall and too thin, we find that the cylinder never falls over onto the diametrically opposite side, as may perhaps be expected from naive symmetry considerations. That is, the old contact point A and the new contact point B on the cylinder’s bottom circular rim are never 180 degrees apart. Fig. 2 shows a histogram of a particular cylinder’s orientations as we repeatedly flicked the cylinder so it falls over onto the other side. The distribution is strongly bimodal with no symmetric falls over many repeated trials. There is clearly a breaking of apparent symmetry.

Is this deviation from symmetry entirely due to our imperfect hands that launched the cylinder? Here we show that the breaking of apparent symmetry is consistent with the simplest deterministic theory, namely smooth non-collisional rigid body dynamics. We derive formulas for the “angle of turn”, the angle subtended by AB at the center of the cylinder’s bottom. These formulas agree well with the casual table-top experiments described above.

II. CANDIDATE THEORIES

If the table were perfectly planar and horizontal, the cylinder’s bottom were perfectly planar, and the cylinder were perfectly axisymmetric, the initial condition with a purely righting angular velocity would result in a collision in which all points on the cylinder’s bottom contact the table-top simultaneously as the cylinder becomes verti-

*Electronic address: msriniva@princeton.edu;
URL: <http://www.tam.cornell.edu/~ms285/>

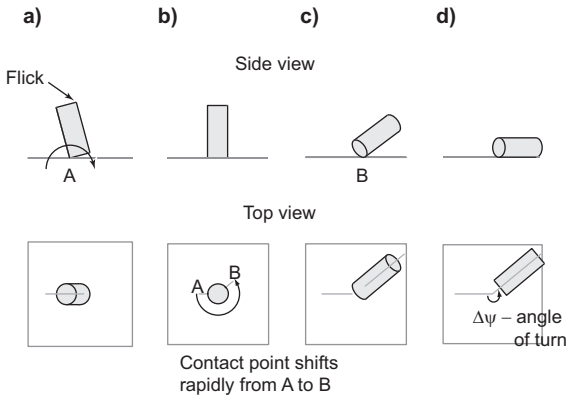


FIG. 1: **Toppling a cylinder** a) Tilt a cylinder and flick its top with your finger, so that b) the cylinder becomes vertical again, but as in c), d) has sufficient energy to fall on to the other side. This schematic shows a time-sequence of cylinder configurations during one such experiment. The cylinder hardly ever falls symmetrically to the diametrically opposite side.

cal. The consequence of such a collision will not be easy to compute since algebraic rigid-body collision laws are not well-defined for truly simultaneous collisions [1]. In any case, this situation of perfectness is physically unlikely for a number of reasons.

Obviously, perfect flatness or planarity is a physically unlikely situation. Some possible geometric perturbations to the cylinder are shown in Fig.3. Say we imagine the cylinder to be solid and as having a nominally flat circular bottom. Then arbitrarily small geometric perturbations, in the form of little bumps on either the cylinder's bottom or the table, will generically lead to an initial two-point collision in this case (current contact point + the small bump on the either surface), and probably result in a cascade of further collisions because of other little bumps on the nominally flat surfaces. The accurate prediction of the detailed consequences of such a cascade of collisions is again hopeless. The consequences of nominally simultaneous point collisions are notoriously sensitive to the ordering of the collisions and other details [2, 3, 4].

On the other hand, we can imagine the cylinder as not being solid, but as having a through-hole. The cylinder's bottom would then simply consist of a circular rim. Geometric perturbations to the circular rim will similarly lead to two-point collisions, where both points of contact are now on the rim. We can then compute the consequences of, say, a plastic collision at the new point of contact. However, the consequences of the collisions will again depend on the location of the geometric imperfection. So such a theory probably cannot be useful in predicting a systematic breaking of symmetry as seen in Fig.2, especially a symmetry-breaking that is invariant to rotations of the cylinder's initial configuration about the cylinder's nominal symmetry axis.

The face-down simultaneous collision is unlikely even

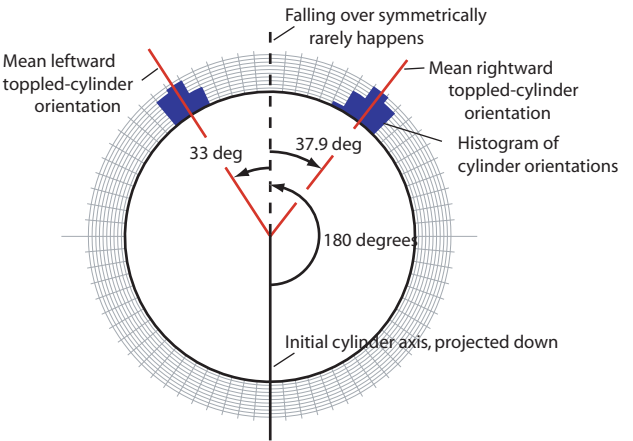


FIG. 2: **Typical toppled cylinder orientations** A histogram on the circle showing the directions along which a particular cylinder aligned itself in a total of 42 separate trials. The cylinder always falls to one side or another, but hardly ever to the diametrically opposite side corresponding to 180 degrees. Whether it falls over to the left or to the right of symmetric depends sensitively on initial conditions. The distribution about 180 degrees is strongly bimodal. The leftward falls have a mean of about 33 degrees and the rightward falls have a mean of about 37.9 degrees from the 180 degree line. Theory predicts an angle of 40 degrees for frictionless sliding and 22 degrees for rolling with no slip.

in the absence of imperfections in geometry and mass distributions. After all, the cylinder is being launched by imperfect human hands that will typically be unable to provide an initial condition that will lead to the face contacting the table. After accounting for various symmetries in the problem, it can be shown that the set of all motions of a cylinder rolling without slip can be characterized by three parameters. However, the set of initial conditions that leads to a face-down collision can be characterized with only two parameters (a set with co-dimension one) [5, 6, 7]. So small generic perturbations of a “collisional” initial condition typically results in a near-collisional motion described entirely by the equations of motion describing the smooth dynamics of the cylinder rolling or sliding on its circular bottom rim. The rest of this paper is about these near-collisional motions – motions that start from initial conditions arbitrarily close to those that lead exactly to a face-down collision. We will see that these near-collisional motions involve rapid albeit continuous rolling or sliding of the cylinder on its bottom rim, so that the contact point appears to have switched by a finite angle, an angle not equal in general to 180 degrees but always greater. For the analysis of these near-collisional motions, we assume geometric perfectness of the cylinder and the table.

A special case of the results in this paper, namely that of a disk rolling without slip and falling almost flat on its face (see section VIII), is discussed from a more sophisticated mathematical perspective in a recent paper [7], published as our paper was being prepared.

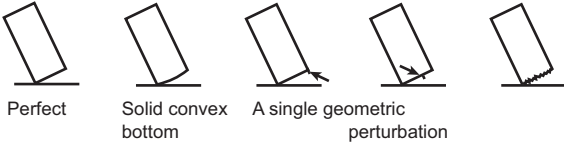


FIG. 3: A variety of geometric perturbations to a cylinder's bottom. Each of these can have drastically different effects on the results of a nominally perfect face down collision. Adapted from [4].

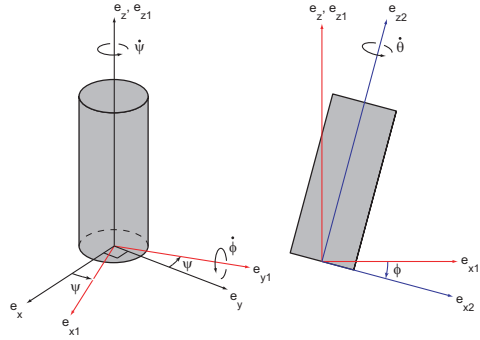


FIG. 4: Definition of the Euler angles and coordinate axes used to define the orientation of the cylinder.

III. DYNAMICS OF ROCKING

Consider a cylinder with mass m , bottom radius R [10], and the center of mass at a height H from the bottom. The moment of inertia is C about its symmetry axis and is A about any axis passing through the center of mass and perpendicular to the symmetry axis. The center of mass of the cylinder is (x_G, y_G, z_G) in an inertial frame $\mathbf{e}_x\text{-}\mathbf{e}_y\text{-}\mathbf{e}_z$ at rest with respect to the table. The reference orientation of the cylinder is vertical as shown in Fig. 4a. Any other orientation of the cylinder can be obtained from the reference orientation by a sequence of three rotations, defining corresponding Euler angles as illustrated in Fig. 4 and angle rates. The first rotation ('yaw' or 'steer') is about \mathbf{e}_z by an angle ψ . This rotation also transforms the inertial coordinate axes to $\mathbf{e}_{x1}\text{-}\mathbf{e}_{y1}\text{-}\mathbf{e}_{z1}$. The second rotation ('pitch' or 'tilt') by an angle ϕ about the \mathbf{e}_{y1} axis results in the $\mathbf{e}_{x2}\text{-}\mathbf{e}_{y2}\text{-}\mathbf{e}_{z2}$ frame and determines the orientation of the cylinder up to a rotation about the body-fixed symmetry axis (\mathbf{e}_{z2} axis). The angular velocity of the cylinder in the rotating $\mathbf{e}_{x2}\text{-}\mathbf{e}_{y2}\text{-}\mathbf{e}_{z2}$ frame is therefore entirely along the symmetry axis \mathbf{e}_{z2} and this relative angular velocity magnitude is denoted by $\dot{\theta}$.

We will consider two simple extremes for the frictional interaction between the table and the cylinder's bottom, namely, sliding without friction and rolling without slip. The equations of motion that determine the evolution of the orientation ψ , ϕ , and θ for a cylinder rolling without slip is described by three second order ODEs:

$$Q_{i1}\ddot{\psi} + Q_{i2}\ddot{\phi} + Q_{i3}\ddot{\theta} = S_i, \quad i = 1, 2, 3. \quad (1)$$

where

$$\begin{aligned} Q_{11} &= A \sin \phi - mHR \cos \phi + mH^2 \sin \phi, \\ Q_{12} &= 0, \quad Q_{13} = -mHR, \\ Q_{21} &= Q_{23} = 0, \quad Q_{22} = -mR^2 - mH^2 - A, \\ Q_{31} &= C \cos \phi + mR^2 \cos \phi - mRH \sin \phi, \\ Q_{32} &= 0, \quad Q_{33} = C + mR^2, \\ S_1 &= (C - 2A - 2mH^2)\dot{\psi}\dot{\phi} \cos \phi + C\dot{\phi}\dot{\theta} \\ &\quad - 2mHR\dot{\psi}\dot{\phi} \sin \phi \\ S_2 &= (C - A + mR^2 - mH^2)\dot{\psi}^2 \sin 2\phi/2 \\ &\quad + (C + mR^2)\dot{\theta}\dot{\psi} \sin \phi + mHR\dot{\psi}\dot{\theta} \cos \phi \\ &\quad + mHR\dot{\psi}^2 \cos 2\phi \\ &\quad + mg(R \cos \phi - H \sin \phi), \\ S_3 &= C\dot{\psi}\dot{\phi} \sin \phi + 2mR\dot{\psi}\dot{\phi}(R \sin \phi + H \cos \phi). \end{aligned} \quad (2)$$

These three equations represent angular momentum balance about the center of mass along the directions \mathbf{e}_{x2} , \mathbf{e}_{y2} , and \mathbf{e}_{z2} , respectively. Because the cylinder rolls without slip, the velocity of the center of mass is entirely determined by the angular velocity and the orientation. Thus, once the angle and the angle rates are known as functions of time, the equations for the center of mass velocity may be integrated to obtain the center of mass position as a function of time.

The equations of motion for a cylinder sliding on its circular bottom rim without friction are also given by Eq. 1 but with

$$\begin{aligned} Q_{11} &= A \sin \phi, \quad Q_{12} = Q_{13} = Q_{21} = 0, \\ Q_{22} &= -A + mHR \sin 2\phi - mH^2 \sin^2 \phi - mR^2 \cos^2 \phi, \\ Q_{23} &= 0, \quad Q_{31} = C \cos \phi, \quad Q_{32} = 0, \quad Q_{33} = C, \\ S_1 &= -2A\dot{\psi}\dot{\phi} \cos \phi + C\dot{\phi}\dot{\theta} + C\dot{\phi}\dot{\psi} \cos \phi, \\ S_2 &= (1/2)(C - A)\dot{\psi}^2 \sin 2\phi \\ &\quad + C\dot{\theta}\dot{\psi} \sin \phi + mgR \cos \phi - mgH \sin \phi \\ &\quad - mHR\dot{\psi}^2 \cos 2\phi + (1/2)m(H^2 - R^2)\dot{\psi}^2 \sin 2\phi, \\ S_3 &= C\dot{\psi}\dot{\phi} \sin \phi. \end{aligned} \quad (3)$$

When the table is frictionless, the horizontal velocity of the center of mass is a constant, so that the horizontal position is independent of the orientation. The vertical position of the center of mass is simply given by $z_G = H \cos \phi + R \sin \phi$. Thus, again, the motion of the center of mass is determined by the evolution of the orientation.

We integrate these equations numerically to see what the near-collision motions look like. We use an adaptive time-step, stiff integrator for the numerical integration. A stiff solver is indicated because we are interested in studying (in hind-sight) solutions that have vastly different time-scales. Also, the fact that the particular Euler-angle description used here is singular at the reference configuration makes the equations stiff when the cylinder is almost vertical. This singularity need not particularly concern us since we are only interested in the near-collisional motions – the equations of motion are always true despite the singularity.

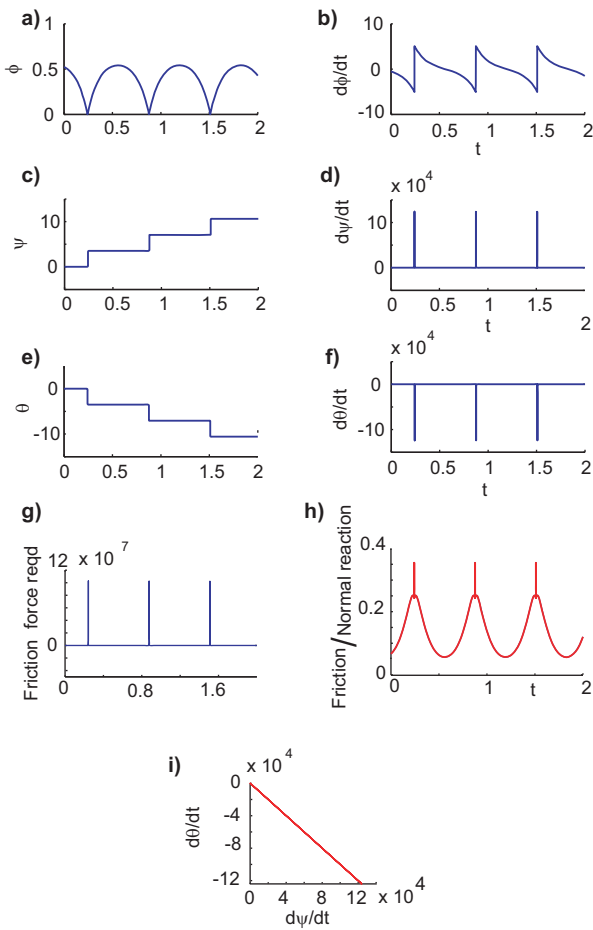


FIG. 5: Results of a typical simulation of a cylinder's face almost but not quite falling flat on the table-top. Physical parameters $m = 1$; $A = 5.1 \times 10^{-3}$; $C = 8 \times 10^{-3}$; $g = 9.8$; $R = 5.1 \times 10^{-2}$; $H = 6.9 \times 10^{-2}$ in consistent SI units. Initial conditions $\psi(0) = 0$, $\dot{\psi}(0) = 0.005$, $\phi(0) = \pi/6$, $\dot{\phi}(0) = -0.5$, $\theta(0) = 0$, $\dot{\theta}(0) = 0.005$. All the angles are in radians.

For simplicity of presentation, we first describe in detail the results of integration when the cylinder does not slip with respect to the table. First, we integrate the equations with initial conditions that lead exactly to a face-down collision $\dot{\psi}(0) = \dot{\theta}(0) = 0$, $\dot{\phi} < 0$, and say, $0 < \phi < \pi/2$. As would be expected, the cylinder rights itself in a manner that all of its bottom face simultaneously reaches the horizontal table-top. The motion of the cylinder is identical to that of an inverted pendulum with the contact point A serving as the pivot point. Having reached the vertical configuration, the cylinder continues to tilt in a pendular manner, penetrating the table-top. This is, of course, because the equations of motion we use do not have any means of detecting and responding to a inter-penetration of two rigid bodies.

The equations of motion here do not have smooth dependence of solutions on initial conditions. Exclusively above-ground motions result from arbitrarily small generic perturbations of these table-penetrating colli-

sional initial conditions. We set $\dot{\psi}(0) = O(\epsilon)$, $\dot{\theta}(0) = O(\epsilon)$, $\dot{\phi} < 0$, and $0 < \phi(0) < \pi/2$, where ϵ is a small quantity. The results of the integration are shown in Fig. 5. The plot of $\phi(t)$ suggests a motion in which the cylinder's bottom face periodically comes close to touching the table ($\phi \rightarrow 0$), but then gets “repelled” by the floor as if by an elastic collision, so that the cylinder rocks down and up periodically, ad infinitum, without losing any energy as would be expected from the conservative equations. We notice that when $\phi \approx 0$, $\dot{\phi}$ changes almost discontinuously. Also, both $\dot{\psi}$ and $\dot{\theta}$ blow up to very large values, resulting in almost discontinuous changes in the corresponding angles ψ and θ when ϕ is close to zero.

Note that we are simply simulating the apparently smooth differential equations, and not applying an algebraic transition rule for a collision. Despite the large angle rates the angular velocity is always bounded, as it must be since energy remains a constant throughout the motion. In particular, while the angle rates $\dot{\theta}$ and $\dot{\psi}$ are large, they are very close to being equal and opposite ($\dot{\theta} \approx -\dot{\psi}$, Fig. 5i).

Let us examine the consequences of a rapid finite change in ψ when $\phi \approx 0$. The position of the contact point (x_P, y_P, z_P) relative to the center of mass (x_G, y_G, z_G) is given by the following equations:

$$\begin{aligned} x_P &= x_G - R \cos \phi \cos \psi + H \sin \phi, \\ y_P &= y_G - R \sin \phi, \\ z_P &= z_G - R \sin \phi \cos \psi - H \cos \phi = 0. \end{aligned} \quad (4)$$

When $\phi \approx 0$ and ψ is not particularly close to any multiple of $\pi/2$, the contact point position is given by

$$\begin{aligned} x_P &\approx x_G - R \cos \psi \\ y_P &\approx y_G - R \sin \psi \\ z_P &\approx z_G - H = 0 \end{aligned} \quad (5)$$

Given that x_G, y_G, z_G do not change much during the brief near-collisional phase (because center of mass velocity is finite), we can see from Eq. 5 that a rapid continuous change in ψ corresponds to a rapid continuous change in the contact point in a circle with the center $O(x_G, y_G, 0)$. Thus the “angle of turn” AOB defined earlier is simply the change in ψ . At the singular limit of a near-collisional motion arbitrarily close to a collisional motion, this continuous but steep change in ψ approaches a step change – this is the “limiting angle of turn” and we denote this by $\Delta\psi_{turn}$.

In summary, we find that the near-collisional motion of the no-slip cylinder can be characterized as being the pasting-together of two qualitatively distinct motions of vastly different time-scales:

1. inverted pendulum-like motion about an essentially fixed contact point when the tilt angle ϕ is large.
2. rapid rolling of the cylinder which accomplishes in infinitesimal time, a finite change in contact point, and a redirection of the downward tilt velocity $\dot{\phi}$ to an equal but opposite upward tilt velocity.

Note that the near-collisional motion for a cylinder rolling without slip requires very high friction forces (Fig. 5g). However, plotting the ratio of the required friction forces with the normal reaction, we find that only a finite coefficient of friction is required for preventing slip even in the collisional limit (Fig. 5h).

The other extreme of exactly zero friction is quite similar. Here, since the horizontal component of the center of mass velocity is a constant due to a lack of friction, we can assume without loss of generality that the horizontal center of mass velocity is zero. Then the near collisional motions for a cylinder sliding without friction can again be characterized as consisting of two qualitatively different phases:

1. a tipping phase when ϕ is not too small, involving the cylinder moving in a vertical plane, the center of mass moving only vertically, and the contact point slipping without friction.
2. a rapid sliding phase in which the sign of $\dot{\phi}$ is reversed almost discontinuously, and the contact point moves by a finite angle in infinitesimal time.

The angle of turn for the frictionless case and the no-slip case are different in general. In the next two sections, we derive the formulas for the angle of turn by taking into account the two-phase structure of the near-collisional motion.

IV. ANGLE OF TURN FOR NO-SLIP ROLLING

The rigid body dynamics of disks, cylinders, and similar objects with special symmetries, have been discussed at length by a number of authors, including distinguished mechanicians such as Chaplygin, Appell, and Korteweg. Their works include complete analytical characterizations of the solutions to the relevant equations of motion, typically involving non-elementary functions such as the hyper-geometric. Reasonable reviews of such literature can be found, for instance, in [5] and [6]. We will not use these somewhat cumbersome general solutions but will analyze only the special near-collisional motion of interest to us.

The calculation below is called, variously, a boundary layer calculation, a matched asymptotics calculation (but we are not interested in an explicit matching) or a singular perturbation calculation. Essentially, we take advantage of the presence of two dynamical regimes with vastly different time-scales, each regime simple to analyze by itself. The overall motion can be obtained approximately by suitably pasting together the small- ϕ and the large- ϕ solutions. But the angle of turn is entirely determined by the small- ϕ regime, as will be seen below.

The equations of motion for no-slip rolling, obviously, conserve total mechanical energy. Also, the total angular momentum $\mathbf{H}_{/G}$ about the line joining the center of mass G and the table-cylinder contact point (say P) is

conserved because both gravity and the contact force always intersect this line by definition. Therefore,

$$\mathbf{H}_{/G} \cdot \mathbf{r}_{PG} = AR\dot{\psi} \sin \phi + CH(\dot{\theta} + \dot{\psi} \cos \phi) \quad (6)$$

$$= b_1, \text{ say.} \quad (7)$$

If we assume initial conditions that almost lead to a face-down collision, $\dot{\psi}(0) = O(\epsilon_1) = \dot{\theta}(0) \ll 1$, we have $b_1 = O(\epsilon_1)$. So rearranging Eq.7, we have:

$$\dot{\theta} + \dot{\psi} \cos \phi = -\frac{RA}{HC} \dot{\psi} \sin \phi + O(\epsilon_1) \quad (8)$$

In the limit of small ϕ , we use $\sin \phi = \phi$ and $\cos \phi = 1$ to obtain

$$\dot{\psi} + \dot{\theta} = -\frac{RA}{HC} \phi \dot{\psi} + O(\epsilon_1). \quad (9)$$

Since $\phi \ll 1$, this equation is the near-unity of the ratio of $\dot{\psi}$ and $\dot{\theta}$ that we noticed in the numerical simulations (Fig.5i).

Now consider Eq.1 with $i = 1$ in the limit of small ϕ , so that we can replace $\sin \phi = \phi$ and $\cos \phi = 1$. We obtain

$$(A - mHR + mH^2)\ddot{\psi} - mHR\ddot{\theta} = (C - 2A - 2mH^2)\dot{\psi}\dot{\phi} + C\dot{\theta}\phi - 2mHR\dot{\psi}\dot{\phi}\phi \quad (10)$$

Using Eq.9 and its time-differentiated version (namely $\ddot{\psi} + \ddot{\theta} = \dots$) in Eq.10 and neglecting higher order terms in ϕ , we obtain:

$$(A + mH^2)\phi\ddot{\psi} = -2(A + mH^2)\dot{\psi}\dot{\phi} \Rightarrow \frac{\ddot{\psi}}{\dot{\psi}} = -2\frac{\dot{\phi}}{\phi} \quad (11)$$

Solving this equation, we obtain

$$\dot{\psi} = \frac{b_2}{\phi^2}. \quad (12)$$

Thus, when $\phi \ll 1$, both $\dot{\psi}$ and $\dot{\theta}$ become very large.

Now consider Eq.1 with $i = 2$ with $\phi \ll 1$.

$$-(A + mR^2 + mH^2)\ddot{\phi} = \dot{\psi}^2\phi(C - A + mR^2 - mH^2) + \dot{\psi}\dot{\theta}\phi(C + mR^2) + mHR\dot{\psi}\dot{\theta} + mHR\dot{\psi}^2 + mgR \quad (13)$$

Using Eq.9 in Eq.13 and again ignoring higher order terms ϕ , we obtain

$$(A + mR^2 + mH^2)\ddot{\phi} = (A + mH^2)\phi\dot{\psi}^2 - mgR \quad (14)$$

Using Eq.12 for $\dot{\psi}$ in the above equation and neglecting the mgR term, we get

$$\ddot{\phi} = \frac{A + mH^2}{A + mR^2 + mH^2} \frac{b_2^2}{\phi^3} \quad (15)$$

$$= \frac{b_3}{\phi^3}, \quad (16)$$

where

$$b_3 = \frac{A + mH^2}{A + mR^2 + mH^2} b_2^2 \quad (17)$$

The general solution for the differential equation in ϕ , Eq.16, can be written as

$$\phi^2 = \phi_c^2 + b_3(t - t_c)^2 / \phi_c^2 \quad (18)$$

where ϕ_c is the lowest ϕ attained by the cylinder before rising back up again, and $t = t_c$ is when this minimum ϕ is attained. Substituting this equation in Eq.12, we obtain a simple equation for the evolution of ψ when near the surface:

$$\dot{\psi} = \frac{b_1}{\phi^2} = \frac{b_2}{\phi_c^2 + b_3(t - t_c)^2 / \phi_c^2} \quad (19)$$

We can now compute the change in ψ during a small time interval Δt centered at $t = t_c$.

$$\Delta\psi_{turn} = \int_{t_c + \Delta t}^{t_c - \Delta t} \dot{\psi} dt \quad (20)$$

$$= \int_{t_c + \Delta t}^{t_c - \Delta t} \frac{b_2}{\phi_c^2 + b_3(t - t_c)^2 / \phi_c^2} dt \quad (21)$$

$$= 2 \frac{b_2}{\sqrt{b_3}} \tan^{-1} \left(\frac{\sqrt{b_3} \Delta t}{\phi_c^2} \right) \quad (22)$$

$$= 2 \sqrt{\frac{A + mR^2 + mH^2}{A + mH^2}} \tan^{-1} \left(\frac{\sqrt{b_3} \Delta t}{\phi_c^2} \right) \quad (23)$$

Suffice it to say that from conservation of energy, we can show that b_2 , and therefore $\sqrt{b_3}$, must be $O(\phi_c)$. Hence, $\sqrt{b_3}/\phi_c^2 \rightarrow \infty$ as $\phi_c \rightarrow 0$. Keeping Δt a small constant as we let $\phi_c \rightarrow 0$, thus approaching the collisional limit, gives us the following expression for $\Delta\psi$.

$$\begin{aligned} \Delta\psi_{turn} &= 2 \sqrt{\frac{A + mH^2}{A + mR^2 + mH^2}} \tan^{-1}(\infty) \\ &= \pi \sqrt{\frac{A + mH^2}{A + mR^2 + mH^2}} \end{aligned} \quad (24)$$

This is the limiting angle of turn when the cylinder rocks by rolling without slip. Earlier numerical integrations agree quite well with this formula in the limit, as they should.

V. ANGLE OF TURN FOR FRICTIONLESS SLIDING

We now briefly outline the procedure for deriving the angle of turn for the frictionless case. The procedure closely parallels that described for the no-slip case, except for small differences below. The frictionless equations Eq.1 and Eq.3 corresponding to $i = 3$ simplifies to

$$\begin{aligned} C \frac{d}{dt} (\dot{\psi} \cos \phi + \dot{\theta}) &= 0 \\ \dot{\theta} + \dot{\psi} \cos \phi &= \text{constant} = b_1, \text{ say.} \end{aligned} \quad (25)$$

Here, as before, $b_1 \ll 1$ because $\dot{\theta}(0)$ and $\dot{\psi}(0)$ are similarly much less than unity by assumption. Using Eq.25 in the frictionless equation Eq.1 and Eq.3 corresponding to $i = 1$, we have, after some simplifications:

$$\begin{aligned} \frac{\ddot{\psi}}{\dot{\psi}} &= \frac{-2\dot{\phi}}{\phi} \\ \dot{\psi} &= \frac{b_2}{\phi^2}. \end{aligned} \quad (26)$$

Substituting this into the $i = 2$ frictionless equation and simplifying by neglecting all higher order ϕ terms, we eventually have

$$\ddot{\phi} = \frac{A}{A + mR^2} \frac{b_2^2}{\phi^3}. \quad (27)$$

This results in the following expression for the angle of turn.

$$\Delta\psi_{turn} = \pi \sqrt{\frac{A + mR^2}{A}}. \quad (28)$$

for the frictionless limit.

VI. QUANTITATIVE COMPARISONS

Firstly and most significantly, note that the limiting angle of turn does not depend on the initial conditions such as the initial tilt and tip velocity. This means that we do not have to control these in an experiment. This also agrees with the relatively small variance in the histogram of Fig.2, in which I did not control the initial conditions.

The histogram Fig. 2 was obtained using a cylinder with $R = 5.1$ cm, $H = 6.9$ cm, $A/m = 5.13 \times 10^{-3}$ m². Using these numbers in the angle of turn formulas gives an angle of turn of about 220 degrees for frictionless sliding and an angle of turn of 202 degrees for rolling without slip. These angles of turn would manifest as a deviation of either 40 degrees or 22 degrees from falling over exactly diametrically. In the toppling experiment of Fig. 2, the cylinder orientation was 33 degrees on average from 180 degrees in the leftward falls (suggesting an angle of turn of 213 degrees) and was about 37.9 degrees on average from 180 degrees in the rightward falls (suggesting angle of turn of 217.9 degrees). The standard deviations were respectively 3.9 and 4.5 degrees respectively. Clearly, neither the frictionless limit nor the no-slip limit is accurate. But both limits capture the many qualitative aspects of the motion quite well. The experimental angle of turn is better predicted by the asymptotic formula for frictionless sliding in this case.

VII. SPECIAL LIMIT: TALL THIN CYLINDERS

For tall thin cylinders with $A \sim mH^2$ and $H \gg R$, both equations for the angle of turn, Eq.24 and Eq.28,

tend to π radians. That is, very tall cylinders are predicted to have a smaller symmetry-breaking. This prediction agrees with the common experience that when we tip a tall-enough cylinder (something that looks more like cylindrical stick or rod) in a manner that its bottom surface falls flat, the cylinder essentially falls over on a contact point diametrically opposite to the initial contact point. Thus this apparent symmetric falling-over is accomplished by a rapid asymmetric rolling or sliding of the cylinder over roughly one half of its bottom rim! And this result seems independent of the cylinder-table frictional properties.

VIII. SPECIAL LIMIT: DISKS

We may define a disk as a cylinder with zero height: $H = 0$. If the radius of gyration of a disk is $R_g = kR$, then $C = mR^2k^2$ and $A = mR^2k^2/2$. Substituting these in either equation for the angle of turn, Eq.24 or Eq.28, we obtain

$$\Delta\psi_{turn} = \pi\sqrt{2 + k^2}/k. \quad (29)$$

Indeed, numerical exploration with a viscous friction-law that spans the range between zero friction and coulomb's law indicates that the angle of turn is independent of the friction law for disks. The formula above for the special case of the near-collisional motion of pure-rolling disks is also derived in a recent paper [7], published as this paper was being prepared.

A homogeneous disk has $k = 1/\sqrt{2}$. The corresponding angle of turn is equal to $\pi\sqrt{5} \approx 2.23\pi$, which is a little (41 degrees) over 360 degrees, a full rotation of the contact point. This prediction is easily confirmed in causal experimentation with metal caps of large-mouthed bottles on sturdy tables – for such bottle caps, we observe that the new contact point is invariably quite close to the old contact point.

A ring such as the rim of a bicycle wheel has $k \approx 1$. The corresponding angle of turn is equal to $\pi\sqrt{3} \approx 1.73\pi$,

which is a little less than 360 degrees (48 degrees). Thus the apparent near-collisional behavior of a homogeneous disk and a ring will be superficially similar, even though the actual angle of turn differ by about 90 degrees.

The angle of turn be controlled by adjusting k . For instance, it is possible to increase the theoretical angle of turn without bound by choosing $k \rightarrow 0$, a disk in which almost all the mass is concentrated at the center. But it would perhaps be hard to experimentally obtain large angles of turn due to frictional losses.

IX. SUMMARY

Here we analyzed what happens when a cylinder or a disk falls flat on its bottom face. We found that the smallest deviation from a perfect face-down collision of a cylinder's bottom results in a rapid rolling and/or sliding motion in which the contact point moves through a finite angle in infinitesimal time. Calculations of this finite angle explain certain apparent symmetry breaking in experiments involving rocking or toppled cylinders.

Flatness and colliding with a flat face is variously degenerate. The consequences of such a degenerate collision can depend sensitively on initial conditions. So, for instance, roboticists that build biped robots simplify control and improve predictability of foot falls by using curved and compliant feet rather than flat rigid feet (e.g., [8]).

Acknowledgments

MS performed these calculations during a graduate dynamics course taught by Andy Ruina. Thanks to Andy Ruina and Arend Schwab for many insightful comments and discussions that have informed this paper immensely. MS was supported by a Cornell University McMullen Fellowship then (Fall 2000). The completion of this manuscript was supported partly by an NSF FIBR grant.

[1] A. Chatterjee and A. Ruina, ASME Journal of Applied Mechanics **65**, 939 (1998).
[2] A. P. Ivanov, Journal of Applied Mathematics and Mechanics **59**, 887 (1995).
[3] S. Goyal, J. M. Papadopoulos, and P. A. Sullivan, Journal of dynamic systems, measurement, and control **120**, 83 (1998).
[4] A. Ruina, J. E. A. Bertram, and M. Srinivasan, Journal of theoretical Biology **14**, 170 (2005).
[5] O. M. O'Reilly, Nonlinear Dynamics **10**, 287 (1996).
[6] A. V. Borisov and I. S. Mamaev, Regular and Chaotic dynamics **7**, 177 (2002).
[7] R. H. Cushman and J. J. Duistermaat, Regular and Chaotic dynamics **11**, 31 (2006).
[8] S. H. Collins, A. Ruina, R. Tedrake, and M. Wisse, Science **307**, 1082 (2005).
[9] A video of this experiment is available from the author's web pages.
[10] Only the bottom radius is important. The cylinder need not have constant radius.